Study of properties of CuO:CR nanostructures thin film

F. Y. Mohammed, Ch. H. Kareem *, F. G. Hammoodi, M. H. Al-Timim
Department of Physics, College of Science, University of Diyala, Iraq

Thin films of polycrystalline CuO were effectively synthesized on pre-cleaned glass substrates through the hydrothermal method. Both undoped and chromium-doped samples were rigorously characterized using X-ray diffraction (XRD), field emission scanning electron microscopy (FE-SEM), energy-dispersive spectroscopy (EDS), and UV–Vis spectroscopy. The results of the XRD analysis confirmed that all films displayed a monoclinic polycrystalline structure, with the doping of chromium affecting the primary crystallite reflections: (110), (002), and (111) for undoped CuO, and (110), (020), and (111) for CuO films doped with 3%, 6%, and 9% chromium. The crystallite sizes, determined using Scherrer's formula, varied from 38.12 nm to 33.26 nm. Analysis of the UV–Vis spectra indicated that the incorporation of chromium modified both the transmittance and the energy band gap, with the Eg values escalating from 1.99 eV for undoped CuO to 3.6 eV for the 9% chromium-doped variant. The FE-SEM imagery demonstrated a smooth and uniform morphology of the films, while EDS analysis verified the presence of chromium as a dopant, along with copper and oxygen. The optical characteristics, encompassing absorbance, transmittance, and band gap energy, were significantly affected by the concentration of chromium.

(Received May 14, 2025; Accepted August 18, 2025)

Keywords: Cr doping, CuO, Thin films, Hydrothermal method, XRD analysis, Optical band gap, FE-SEM

1. Introduction

The distinctive characteristics and structural variability of metal oxide nanostructures have garnered significant scientific attention for several nano-applications, including electronics, catalysis, optics, optoelectronics, and biosensing [1]. In the realm of metal oxide semiconductors, CuO nanofilms have become a significant study focus owing to their exceptional physicochemical features. CuO is a p-type semiconductor with intriguing features, including a direct energy band gap between 1.1 and 2.1 eV [2]. The synthesis of diminutive CuO nanoparticles with distinct geometries (e.g., nanorods or nanowires) has garnered the interest of researchers owing to their remarkable performance and distinctive features [3]. Therefore, it has become necessary to study different synthetic approaches to regulate the form, size, and phase of CuO nanostructures to accomplish technological improvement. Too far, a number of techniques have been employed to generate CuO nanostructures, including hydrothermal methods [4], oxidation processes [5], spray pyrolysis [6], sonic emulsions, thermal evaporation, electrochemical approaches, and precipitation [7,8]. Each of these approaches has unique advantages and challenges, including high cost, complexity, and synthesis time, in addition to potential issues associated with the use of surfactants or templates and elevated synthesis temperatures, which can negatively impact process efficiency and economics [9]. CuO nanocrystals have been manufactured by a hydrothermal technique employing precursors such as copper acetate dihydrate, copper nitrate hexahydrate, and hexamethylenetetramine. The precursor solution is reacted in an autoclave at high pressure and high temperature (120 °C) for a long duration (12 h). The approach reported by Yu et al. requires two weeks to synthesis CuO nanostructures; Laksa et al., however, have presented similar synthetic methods. & Jiang et al. created copper oxide nanowires by thermally oxidizing a copper substrate at high temperatures (400 to 700 °C) in air. Cr doping may greatly increase the surface

* Corresponding author: chiahaseeb@uodiyala.edu.iq
https://doi.org/10.15251/DJNB.2025.203.965

shape, donor density, surface charge, incidence of oxygen vacancies, and catalytic activity of CuO. This doping procedure is especially useful for semiconductor materials since the inclusion of chromium may drastically influence the characteristics of CuO, impacting numerous parameters such as ammonia detection, transmittance, and optical bandgap. Pat et al. produced Cr-doped CuxO thin films using a thermal ionic vacuum arc plasma method, displaying outstanding transparency and dielectric constant. Recent improvements include the deposition of transition metal oxides to increase the crystalline quality of CuO films. Although various research groups have explored the physical and chemical characteristics of doped CuO films [10,11,12], the extant literature on Cr-doped CuO films is quite limited. The emphasis of this work is on the synthesis of Cr-doped CuO films utilising a conventional process that is easy, environmentally benign, and suitable to growth across a broad range of area sizes.

2. Experimental

2.1. Preparation of CuO seed layer

The solution was produced by dissolving copper acetate dihydrate (Cu (CH3COO)2·H2O) at a concentration of 10 mM in 50 ml of ethanol and sonicating for 15 minutes. The solution was then sprayed to a new glass substrate at a temperature of 100 degrees Celsius using a spray technique of deposit. The settings that were optimized for the process comprised a spray duration of 10 seconds, an average deposit rate of 10 cm3/min, a distance of 30 cm between the nozzle and the substrate, and filtered compressed air as the gas that was utilized to carry the process. The pressure of the process was maintained at 105 Nm-2. The rise in size of copper oxide (CuO) films was assisted using a hydrothermal technique. Ultimately, all films were tempered on a hot plate at a temperature of 250°C for 2 hours and 30 minutes in an air environment.

2.2. Growth of CuO: Cr

After depositing the CuO seed layer, the seed substrate was put vertically in an autoclave holding the growth solution and heated to a temperature of 120°C in an oven for 10 h, ensuring that the seed layer substrate was looking downwards. The solution for growth was produced by mixing 30 mM of $C_6H_{12}N_2$, Cr (NO3)3, and Cu (NO3)6 in 50 ml of deionized water and sonicating for 15 minutes. The concentrations of chrome and copper oxide were set to generate films of varied composition, namely, undoped, 3% Cr, 6% Cr, and 9% Cr. After the culture procedure, the produced films were gently washed with deionized water in order to eliminate the salt from their surface that was bonded to them. Ultimately, all of the films were tempered on a hot plate at 400 degrees Celsius for two hours.

3. Results and discussion

3.1. Structural characterization

X-ray diffraction was applied to analyze the composition and structure of the Cr-doped CuO films. A Cu Kα source of radiation (λ = 0.154187 nm) was utilized, it operated at 40 keV and 30 mA at the ambient temperature with 2θ values ranging from 20° to 65°. The patterns obtained from the XRD studies for the samples containing undoped CuO, 3% Cr doped CuO, 6% Cr doped CuO, and 9% Cr doped CuO are presented in Figure 1. These patterns feature a distinctive monoclinic structure, which is particular to CuO. The peaks that are seen at (110), (002), (111), and (020) are attributable to the CuO phase (ICDD 00-005-0661) [13,14]. The precise patterns of diffraction in the spectra suggest that the films are formed of pure CuO. Additionally, the variation of the doping ratio modified the XRD patterns of the coated films, which revealed that structural changes occurred as a consequence of the Cr (3%), Cr (6%), and Cr (9%) doping. Previous research has demonstrated variations in the parameters of crystallinity related with an increase in the Cr concentration. Changes in the characteristics of crystallites due to doping of metal ions in CuO have previously been observed by various groups of researchers.[15]. Specifically, the location of the (110) plane in the initial film of CuO was displaced to narrower angles of

diffraction owing to doping with Cr. This event illustrates the success of the doping procedure, as the peak location is changed inside the film's substance owing to the differing sizes of ions in the dopant and the host metal (Cr2+: 0.73 Å, Cu2+: 0.57 Å; coordination number 6).[16].

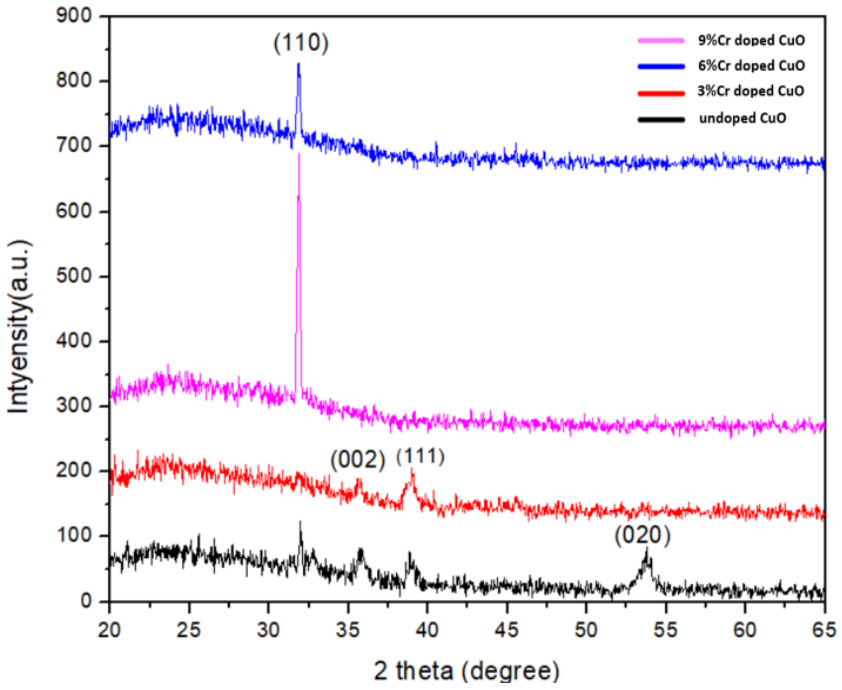

Fig. 1. The XRD patterns of un-doped and Cr-doped CuO films on glass substrate are displayed.

The lattice parameters (and associated coefficient) are derived from the following equation.[17]

$$d_{hkl} = \frac{a}{\sqrt{4/3 \quad h^2+k^2+hk+\frac{l^2 a^2}{c^2}}} \tag{1}$$

The size of the crystallite (D) was computed using the width of the corner at the complete length of the (110) plane, using the following formula. [18].

$$D = \frac{K\lambda}{\beta cos\theta} \tag{2}$$

where ***D*:** The size of the crystal, stated in terms of its longest dimension, is λ= 1.5406 A°, β its beta value is 1.5406 A°, and its diffraction angle θ is 1.5406 A°.

The examination of the crystal size of Cr-doped CuO films that were subjected to 400 degrees Celsius for two hours indicated that the D value altered with Cr doping.

The number of defects present in the sample (δ) is assessed using the corresponding equation [19]:

$$\delta = \frac{1}{D^2} \tag{3}$$

In the context of dislocation density (denoted as δ), it has been demonstrated that the value of δ is proportional to the square of the value of D.

The duration of the elongation period is regulated by the concentration of the Cr dopant. As a consequence, it is believed that the principal impact of modifying D is derived from the strain's variance. Dulay et al. revealed that Cr-doped CuO films displayed a drop in strain values

with concentration changes, this was caused by a decrease in D that led to strain relaxation. The fluctuation of strain was measured for every movie using the provided formula [20]:

$$\varepsilon = \frac{\beta}{4tan\theta} \tag{4}$$

The data collected using X-ray diffraction (XRD) that comprises the values of tip orientation, strain (ε), crystal size (D), dislocation density (δ), and interplanar spacing (d-spacing), is given in Table 1.

Table 1. The calculation of structural parameters based on the dislocation density at the (110) peak position.

Samples	D (nm)	d_{hkl}	strain	Dislocation Density δ x 10^{15} m^{-2})
CuO-Undoped	38.12	2.79575	11.6149	0.688
CuO:Cr(3%)	8.62	2.79623	51.3255	13.458
CuO:Cr(6%)	41.15	2.80572	10.7949	0.590
CuO:Cr(9%)	33.26	2.80541	13.3546	0.903

3.2. FE-SEM analysis

The physical features of the films were examined using field emission scanning electron microscopy (FE-SEM), as indicated in Figure 2. The granules are regularly spaced, and the surface of the film is barely smooth. This ordered grain structure is particularly obvious in the Cr-doped CuO and pure CuO films, which is induced by the creation of the compound. The CuO:Cr crystals are rod in form, and all grains have a similar description; these photos illustrate the distribution of size and surface properties seen for tiny particles on the film. These nanorods fully envelop the surface, which implies that they have a substrate that is nanorods. The average diameter of the (CuO) films was assessed using Image J software, and the findings reveal that modifying the doping ratio has varied impacts on the average diameter of the films. Specifically, the average diameter was shown to decrease with increasing Cr doping levels (0%, 3%, 6%, and 9%) (to 61, 60, 42, and 40nm, respectively). Figure 2 illustrates the FE-SEM picture of the cross section of the 3%Cr-doped CuO film, whereas Figure 3 presents the FE-SEM images of the undoped CuO and Cr-doped CuO films.[21]

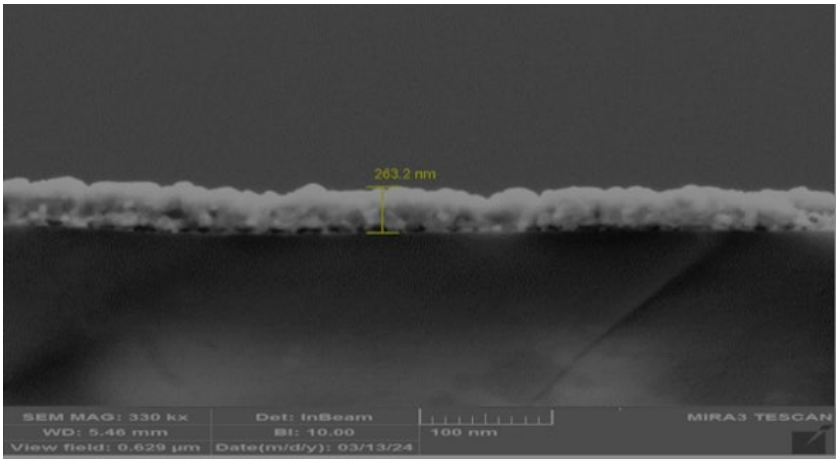

Fig. 2. The FE-SEM picture shows the cross section of a 3% Cr-doped CuO film.

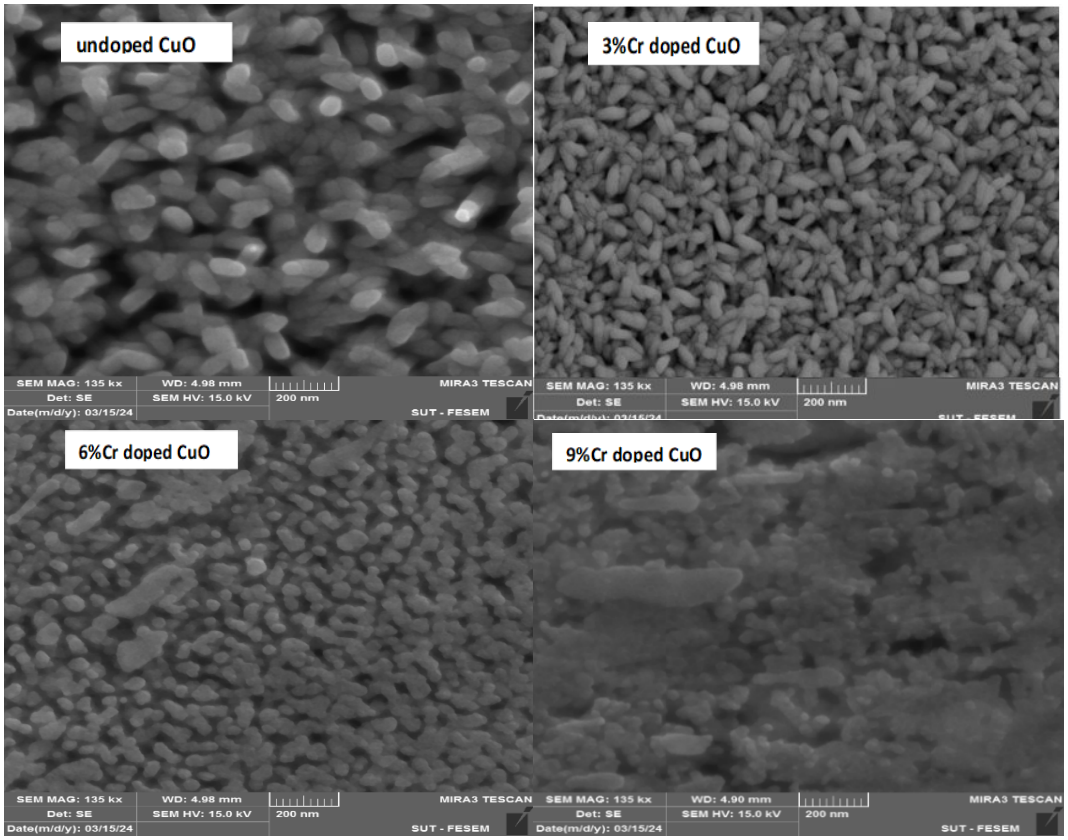

Fig. 3. FE-SEM pictures of unoped CuO and Cr-doped CuO films that lacked doping.

3.3. EDS analysis

Energy dispersive spectroscopy (EDS) is a chemical analysis technique that utilizes an electron beam (10 keV) to identify the chemical or elemental makeup of a sample. The approach is developed from the interaction between an X-ray source and the thing being investigated. The characteristic of EDS is the ability to discriminate components.

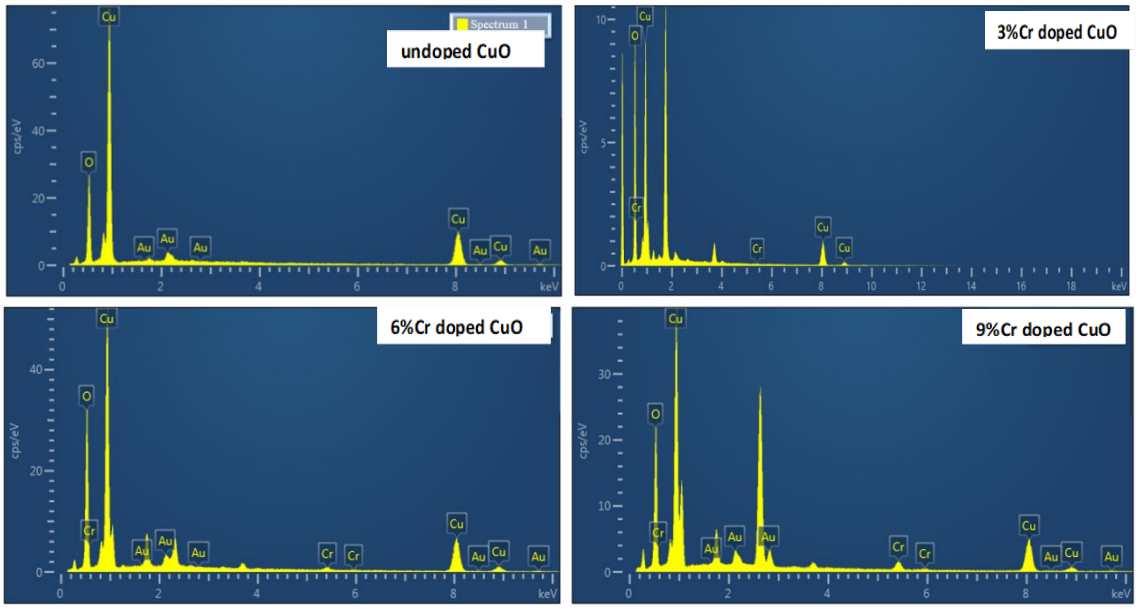

Fig. 4. EDX spectrum of undoped CuO and Cr doped CuO thin films.

This is derived from the premise that each element has a distinct atomic composition that creates a specific spectrum of peaks that may be noticed in its electromagnetic emission. The EDS technique was applied to confirm the chemical composition of copper (II) oxide (CuO). The EDS spectrum of CuO in Figure 4 demonstrates that all of the elements present in the film, including Cr, Cu, and O, are compositionally connected with the film. For the Cr-doped samples, the composition of elements is confined to Cu, Cr, and O. The composition of the 3%, 6%, and 9% Cr-doped CuO samples is reported in Table 2 [22].

Table 2. Composition analysis of 3%, 6% and 9% Cr-doped CuO samples.

	Undoped CuO	**CuO:Cr(3%)**	**CuO:Cr(6%)**	**CuO:Cr(9%)**
Element	Wt%	Wt %	Wt%	Wt %
O	20.80	41.39	29.48	26.49
Cu	79.20	58.39	68.87	67.88
Cr	0	0.23	1.65	5.62
Total	100.00	100.00	100.00	100.00

3.4. Optical Properties of CuO

The optical band gap (E_{gap}) is a material property that is intrinsic to all substances, and can be altered by adding foreign atoms to the material's lattice composition. Measuring this property is accomplished by exciting electrons across the valence conduction band at a specific frequency. When the primary absorption threshold is reached, the optical transition is decided by utilizing the classical equation for calculating the band gap energy (E_{gap}) [23].

$$\alpha h\nu = B\,(h\nu - E_{gap})^{r} \tag{5}$$

In this case, B is the tail's band's constant, hv is the photon's energy, and r is the direct band's gap, which is depending on the crystalline or amorphous nature of the material. The classification of the band gap is based on the value of m, and is as follows: direct transitions that are directly permitted have a value of 2, while indirect transitions that are permitted have a value of 1/2; direct transitions that are forbidden have a value of 3, and indirect transitions that are forbidden have a value of 3/2. To calculate the Egap of pure CuO and Cr-doped CuO films, plots of $(\alpha h\nu)^2$ against (hv) were generated as depicted in Figure 5.

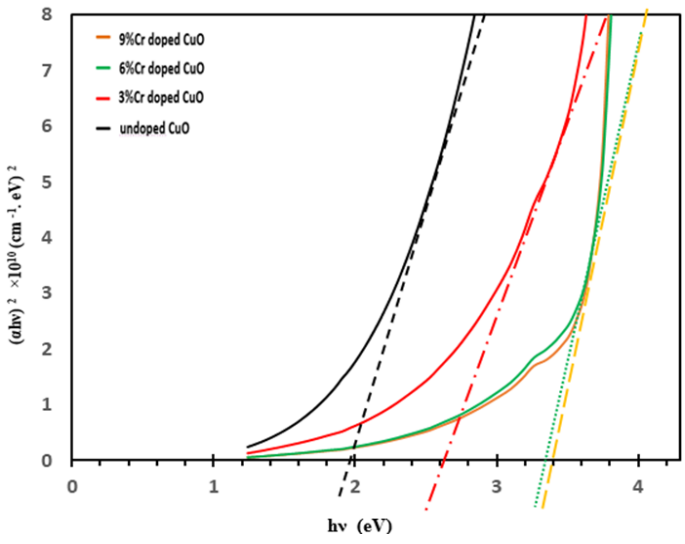

Fig. 5. Optical bandgap assessments for pristine CuO and chromium-doped CuO thin films.

The linear connection between these (αhν)2 and (hν) plots permitted the direct measurement of the film's band gap directly (Egap). The values of the band gap energy (Eg) found were: 1.99 eV for pure CuO, 2.61 eV for 3% Cr doped CuO, 3.56 eV for 6% Cr doped CuO, and 3.6 eV for 9% Cr doped CuO.

Figure 6 demonstrates the link between the absorbance coefficients of pure CuO and Cr-doped CuO thin films that are formed on glass substrates. The findings reveal that the absorption coefficient of the Cr-doped CuO layer is lower at longer wavelengths. Additionally, the rise in Cr-doping causes the absorption coefficient to grow shorter, as indicated by the reduction in the measured value of the absorption coefficient. The modifications in the absorption characteristics of CuO thin films imply their prospective utilization in varied sectors, including photovoltaic devices [24].

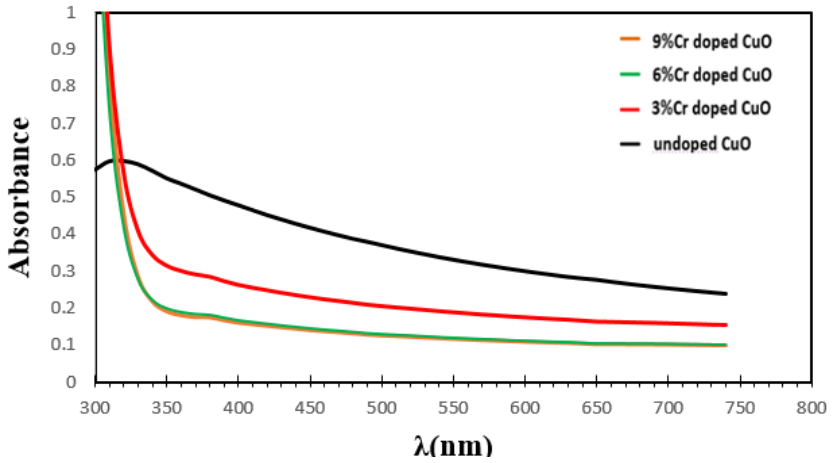

Fig. 6. The fluctuation in absorbance for both virgin CuO and chromium-doped CuO films is depicted as a function of (λ).

Article 7 This article explains the optical transmission of pure copper oxide (CuO) thin films and the optical transmission of chromium-doped copper oxide (CuO) thin films for the purpose of optical research. The room temperature transmission spectra of these layers was measured in the region of 300-800nm. The findings reveal that pure CuO has a poor transmission below 700nm, and a boost in transmission beyond 700nm. In contrast, the chromium-doped CuO has a greater range of transmission, the greatest transmission is recorded at 800nm.

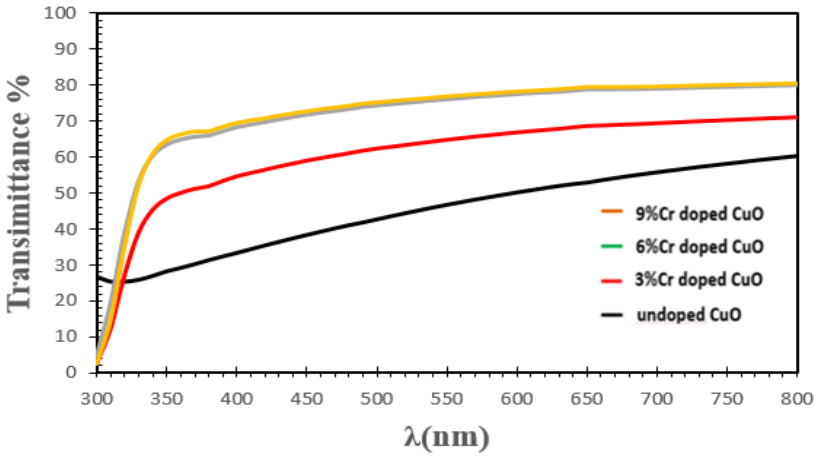

Fig. 7. The transmission spectra of unoped and Cr doped copper oxide thin films are presented in the figure.

5. Conclusions

Ultimately, CuO nanorod arrays were generated utilizing a hydrothermal technique, these treatments comprised varied concentrations. The X-ray diffraction (XRD) data indicated that the films were polycrystalline and contained a monoclinic structure. It was discovered that the full width at half maximum (FWHM) of the films increased with doping, which is suggestive of a reduction in grain size. Morphological tests employing field emission scanning electron microscopy (FE-SEM) indicated that the deposited films were smooth and had a uniform surface. Additionally, energy dispersive spectroscopy (EDS) study indicated that Cr doping affected the distribution of grains and confirmed that all constituent components are present in the films. Additionally, optical investigations indicated that Cr doping in pure CuO films may considerably boost the absorption and transmission of light as well as the optical band gap.

Acknowledgements

The author extends his sincere thanks to the University of Diyala, Iraq, for providing the academic environment that supported the completion of this research. Although this work did not receive any specific financial support, their intellectual and moral contributions were essential to its success.

References

[1] Hansen, B. J., Kouklin, N., Lu, G., Lin, I. K., Chen, J., Zhang, X. (2010), Journal of Physical Chemistry C, 114(6), 2440-2447; https://doi.org/10.1021/jp908850j

[2] Jassim, D. N., Mansour, J. M., Mohammed, G. H. (2024), Journal of Optics, 1-11; https://doi.org/10.1007/s12596-024-02247-5

[3] Kareem, M. M., Khodair, Z. T., Mohammed, F. Y. (2020), J. Ovonic Res., 16(1), 53-61; https://doi.org/10.15251/JOR.2020.161.53

[4] Kareem, M. M., Mohammed, F. Y., Khodair, Z. T. (2021, May), Journal of Physics: Conference Series (Vol. 1879, No. 3, p. 032090). IOP Publishing; https://doi.org/10.1088/1742-6596/1879/3/032090

[5] Kiwi, J., Pulgarin, C., Peringer, P. (1994), Applied Catalysis B: Environmental, 3(4), 335-350; https://doi.org/10.1016/0926-3373(94)00008-5

[6] Hameed, S. A., Kareem, M. M., Khodair, Z. T., Saeed, I. M. M. (2021), Chemical Data Collections, 33, 100677; https://doi.org/10.1016/j.cdc.2021.100677

[7] Anandan, S., Wen, X., Yang, S. (2005), Materials Chemistry and Physics, 93(1), 35-40; https://doi.org/10.1016/j.matchemphys.2005.02.002

[8] Bayal, N., Jeevanandam, P. (2012), Journal of alloys and compounds, 537, 232-241; https://doi.org/10.1016/j.jallcom.2012.05.086

[9] Wang, Z. L. (2006), Metal and semiconductor nanowires. (No Title).

[10] Ishihara, T., Higuchi, M., Takagi, T., Ito, M., Nishiguchi, H., Takita, Y. (1998), Journal of Materials Chemistry, 8(9), 2037-2042; https://doi.org/10.1039/a801595c

[11] Kumar, K., Chowdhury, A. (2017), Ceramics International, 43(16), 13943-13947; https://doi.org/10.1016/j.ceramint.2017.07.125

[12] Baturay, S., Candan, I., Ozaydın, C. (2022), Journal of Materials Science: Materials in Electronics, 33(9), 7275-7287; https://doi.org/10.1007/s10854-022-07918-2

[13] Lu, P., Wu, P., Wang, J., Ma, X. (2019), Chemical Physics Letters, 730, 297-301; https://doi.org/10.1016/j.cplett.2019.06.029

[14] Obulapathi, L., Kumar, A. G., Sarmas, T. S., Rao, T. S. (2014), International Journal of Nanotechnology and Application (IJNA), 4(4), 29-34.

[15] Gezgin, S. Y., Baturay, Ş., Candan, İ., Kılıç, H. Ş., Middle East Journal of Science, 9(2), 67-81; https://doi.org/10.51477/mejs.1288533

[16] Dinc, S., Şahin, B., Kaya, T. (2020), Materials Science in Semiconductor Processing, 105, 104698; https://doi.org/10.1016/j.mssp.2019.104698

[17] Yu, L., Zhang, G., Wu, Y., Bai, X., Guo, D. (2008), Journal of Crystal Growth, 310(12), 3125-3130; https://doi.org/10.1016/j.jcrysgro.2008.03.026

[18] Hammoodi, F. G., Shuihab, A. A., Ebrahiem, S. A. (2022, November), AIP Conference Proceedings (Vol. 2394, No. 1). AIP Publishing; https://doi.org/10.1063/5.0122507

[19] Shaikh, J. S., Pawar, R. C., Devan, R. S., Ma, Y. R., Salvi, P. P., Kolekar, S. S., Patil, P. S. (2011), Electrochimica Acta, 56(5), 2127-2134; https://doi.org/10.1016/j.electacta.2010.11.046

[20] Paul Joseph, D., Venkateswaran, C., Sambasivam, S., Choi, B. C. (2012), Journal of the Korean Physical Society, 61, 449-454; https://doi.org/10.3938/jkps.61.449

[21] Kambale, S. V., Lokhande, B. J. (2023), Materials Chemistry and Physics, 295, 127166; https://doi.org/10.1016/j.matchemphys.2022.127166

[22] Dinc, S., Şahin, B., Kaya, T. (2020), Materials Science in Semiconductor Processing, 105, 104698; https://doi.org/10.1016/j.mssp.2019.104698

[23] Hammoodi, F. G., Shuihab, A. A., Ebrahiem, S. A. (2022, November), AIP Conference Proceedings (Vol. 2394, No. 1). AIP Publishing; https://doi.org/10.1063/5.0122507

[24] Dolai, S., Dey, R., Das, S., Hussain, S., Bhar, R., Pal, A. K. (2017), Journal of Alloys and Compounds, 724, 456-464; https://doi.org/10.1016/j.jallcom.2017.07.061